Journal of Hydrology: Regional Studies 47 (2023) 101404

Contents lists available at ScienceDirect

Journal of Hydrology: Regional Studies

journal homepage: www.elsevier.com/locate/ejrh

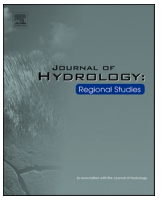

A combined index to characterize agricultural drought in Italy at municipality scale

Lauro Rossi [a,*], Gustavo Naumann [a], Simone Gabellani [a], Carmelo Cammalleri [b]

[a] CIMA Research Foundation, Via Magliotto 2, Savona, Italy
[b] Politecnico di Milano, Piazza Leonardo da Vinci, 32, Milan, Italy

ARTICLE INFO

Keywords:
Drought monitoring
Drought impact assessment
Combined drought indicator
Agricultural drought

ABSTRACT

Study region: Italy and in particular the provinces of Verona and Foggia.
Study focus: The assessment of drought impacts at local scale requires adequately detailed spatio-temporal estimates of drought severity. Given the intrinsic uncertainty in drought severity estimates based on a single index, especially at high spatial resolution, the use of combined indices is preferable. However, the disagreement between the single indices needs to be addressed. We propose a methodology to combine the Standardized Precipitation-Evapotranspiration Index and the Soil Moisture Anomalies based on a double-entry matrix. The classification adopted to define five semi-quantitative severity classes is generalized by introducing an objective approach to assign values when the two base indices disagree. The methodology is tuned over two Italian provinces, Verona and Foggia, with focus on agricultural drought at the high spatial detail of single municipalities.
New hydrological insights for the region: The methodology is proved to be skillful (Heidke Skill Score of 0.75) in capturing the spatio-temporal evolution of the major agricultural droughts observed in the two case study regions (2012, 2015 and 2017), which are benchmarked using data from drought impact databases. The temporal dynamics modeled by this index align with the timeline of the drought events, suggesting that the index is suitable for near-real time agricultural drought monitoring. The simplicity of the double-entry matrix approach allows for upscaling to the entire country.

1. Introduction

Agriculture is one of the socio-economic sectors that is more vulnerable to drought events (FAO, 2021) due to the direct dependence of rainfed plant productivity to climate variability (Riha et al., 1996), and the destabilization in water resource partitioning caused by increasing irrigation demand during periods with limited water availability (e.g., De Stefano et al., 2015; Venezian Scarascia et al., 2006). In Italy, drought-induced economic losses in the agriculture sector were estimated to be between 0.55 and 1.75 billion euro in 2011–2016 (García-León et al., 2021). Coldiretti, the main Italian association of agricultural sector managers, have reported an impact of about 2 billion euros of the drought in 2017 for the Italian agriculture sector (https://www.coldiretti.it/economia/istat--clima-pazzo-taglia-la-produzione-alimentare), and estimated that losses for the recent 2022 drought in northern Italy are in a similar, if not higher, order of magnitude (https://www.coldiretti.it/economia/siccita-il-conto-dei-danni-sale-a-3-mld-sos-raccolti, last access

* Corresponding author.
E-mail address: lauro.rossi@cimafoundation.org (L. Rossi).

https://doi.org/10.1016/j.ejrh.2023.101404
Received 19 December 2022; Received in revised form 6 April 2023; Accepted 27 April 2023
Available online 3 May 2023

28/3/2023).

These recent disastrous events have increased the awareness on the need to build capacity to adapt and mitigate drought risk, as numerous call-for-action initiatives supported a shift in drought management paradigm toward a more proactive approach (UNDRR, 2021). WMO and GWP (2014) have introduced a three pillars strategy for an integrated management of drought, in which drought monitoring and early warning systems (DEWS) play a key role to increase preparedness.

Drought indices constitute the core of any DEWS, aiming at capturing the spatio-temporal evolution of the main drivers of drought, and often specialized in identifying a specific type of drought (WMO and GWP, 2016). There are numerous drought indices specifically designed to reproduce the effects on agriculture, ranging from meteorological-based indices (i.e., Palmer Drought Severity Index, PDSI, and Standardized Precipitation Evapotranspiration Index, SPEI; Alley, 1984; Vicente-Serrano et al., 2010), indices focusing on the quantification of water stress (soil moisture anomalies, SMA, drought severity index, DSI, and Evaporative stress Index, ESI; Anderson et al., 2011; Cammalleri et al., 2016), or directly monitoring the greenness of the vegetation (Vegetation Condition index, VCI, and fraction of Absorbed Photosynthetically Active Radiation, fAPAR; Kogan, 1995; Peng et al., 2019).

The large array of indices available in the scientific literature is not only dictated by the lack of consensus in the drought community on the definition of a univocal index for agricultural drought, but it is intrinsically connected to the complexity of the phenomenon, the specificity of drought dynamics over different regions, and by the consequent uncertainty associated to the estimates of drought severity performed by a single index (Hoffmann et al., 2020). For this reason, combined indices have been proposed in the literature to merge the information provided by multiple base indices, aiming at strengthening the assessment by exploiting converge of evidence (Leeper et al., 2022). The different combination strategies range from a simple average of the various base indices (Crow et al., 2012), only for indices with comparable ranges of variability, to the use of copula functions (Hao and AghaKouchak, 2013), which require extensive datasets for the fitting, and it can be computationally intense.

In the framework of risk analysis, it is well-established the use of double-entry matrix as a powerful tool to characterize risk under uncertainty (Jordan et al., 2018). This approach has the advantage of allowing for a large degree of flexibility in the definition of the outcome based on the combination of the two inputs, which is a useful feature especially in the case of disagreement between the indices. The same approach can be adopted to combine drought severity indices.

At continental and global scale, with coarse spatial resolution models, both single and combined drought indices are used to characterize drought severity in risk analyses (e.g., Meza et al., 2020), as well as to build large-scale damage functions (Naumann et al., 2015). While those studies may be useful in supporting the development of long-term adaptation measures at continental, national- and sub-national scale, agricultural drought monitor requires more spatially detailed information, based on high-resolution data and ad-hoc analyses. Given the current lack of a high-resolution drought monitoring system at national level, the aim of this study is to develop and test a drought-severity combined index able to characterize agricultural drought conditions in Italy at the detailed spatial scale of the single municipalities. The goal is two-fold: 1) to develop a combined index based on an objective (non-arbitrary) methodology to merge two base indices (SPEI and SMA) using a double-entry matrix approach; 2) to evaluate the performance of the proposed combined index using high resolution data (500-m to 1-km) suitable for municipality-scale applications during recent documented agricultural drought events in Verona and Foggia Provinces.

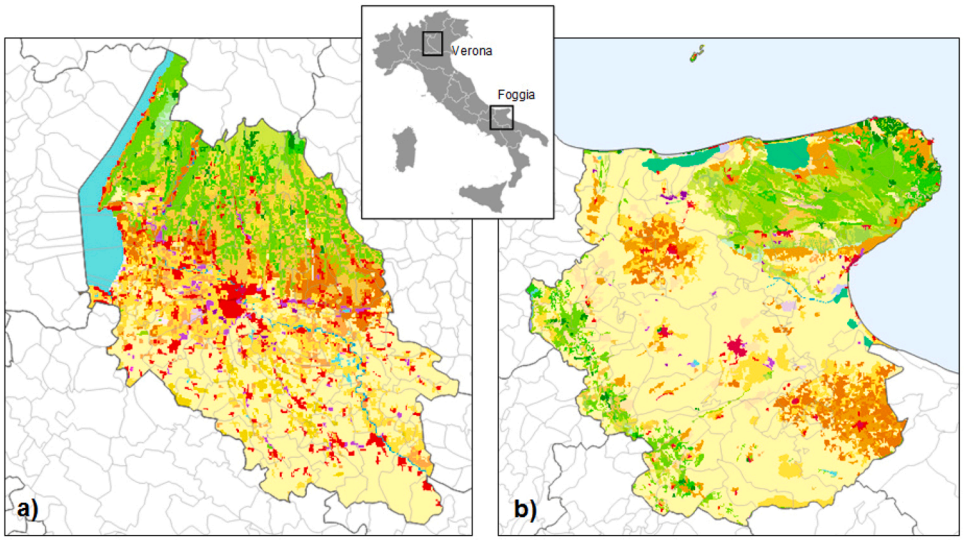

Fig. 1. Location of the two study areas (see insert), and spatial distribution of the land cover classes according to Corine land cover map for: (a) Verona, and (b) Foggia. Agricultural areas are depicted in yellow to brown shades (see https://land.copernicus.eu/pan-european/corine-land-cover/clc2018 for the full legend of the classification).

2. Data and methods

2.1. Study area

The combined index is developed and tested over two provinces in Italy, Verona in western Veneto and Foggia in northern Apulia, selected as representative of different climate conditions, morphology and agricultural practices of the Italian territory (see Fig. 1).

The Verona province is located in north-eastern Italy and includes 98 municipalities. It is characterized by cold temperatures in the winter and warm and humid summers (humid subtropical, *Cfa*, following the Köppen classification). The average annual temperature is between 13 and 14 °C. Precipitation is evenly distributed thought the year, with annual average precipitation between 700 and 800 mm, and the rainiest period being between September and November. From an agricultural standpoint, the region is renowned for its vineyards, even if other cultivars are also important, such as apples, cherry, corn and sugar beet.

The Foggia province is located on the south-eastern coast of Italy, overlooking the Adriatic Sea, and it comprises 61 municipalities in three distinct regions: the central region, *Tavoliere*, where the city of Foggia is located, the coastal region, *Gargano*, and the Appennines area. Most of the province is characterized by a typical Mediterranean climate (hot-summer Mediterranean, *Csa*, in the Köppen classification), with warm, dry summers, and temperatures often reaching 40 °C. Precipitation falls mainly in late autumn and winter, with an annual average between 450 and 600 mm (with the exception of mountain areas where rainfall is much higher). The central section of the province is an important agricultural area, with one of the major Italian productions of wheat, and other important species such as grapefruit, olives and tomato.

2.2. Drought indices

Agricultural drought conditions are generally described as a reduction in soil water availability for the plants (and consequent increase in the water stress), which is associated to the combined effects of a reduction in the water supply (i.e., precipitation) and/or an increase in the atmospheric water demand (i.e., evapotranspiration). For this reason, two commonly used agricultural drought indices are here proposed as a starting point for the combined index: i) the Standardized Precipitation-Evapotranspiration Index (SPEI, Vicente-Serrano et al., 2010), and ii) the standardized soil moisture anomaly (SMA, Cammalleri et al., 2016; Sheffield and Wood, 2007).

The SPEI is defined in analogy to the Standardized Precipitation Index (SPI, McKee et al., 1993) but using as input the difference between precipitation and potential evapotranspiration rather than only the precipitation. A theoretical probability distribution is fitted on a historical time series of the data, commonly the Log-logistic distribution, and the probability is converted in a standard normal value (centered on 0 and with a unitary standard deviation). In this study the precipitation and potential evapotranspiration data from the BIGBANG database (Braca et al., 2021) are used to compute the SPEI at 3-month accumulation period (SPEI-3). The dataset is openly available at https://groupware.sinanet.isprambiente.it/bigbang-data/library/bigbang40 (last access 28/03/2023), and it includes monthly maps at 1-km spatial resolution of precipitation, interpolated from more than 2500 ground stations included in the DBPLUVIOM 4.0 database using the natural neighbors 2 step method, and potential evapotranspiration, derived from monthly temperature maps (interpolated through regression kriging) using the Thornthwaite (1948) method. Since this dataset covers a period up to the year 2019, the Log-logistic distribution is fitted on a reference period 1990–2019, only slightly different that the period 1991–2020 recommended by the World Meteorological Organization as a standard for monitoring (WMO, 2017).

The SMA is computed by fitting a Beta-distribution to monthly soil moisture values in the root zone (Cammalleri et al., 2016; Sheffield and Wood, 2007) and expressing the probability as a standardized normal quantity. This index is based on the outputs of the hydrological model Continuum, fully described in Silvestro et al. (2013) and (2015), which has been used for many research studies on hydrological extremes (e.g., Laiolo et al., 2016; Silvestro et al., 2016 and 2019; Cenci et al., 2016; Corral et al., 2019; Poletti et al., 2019). The model solves both the mass and the energy balances on a regular square mesh using a force-restore approach (Dickinson, 1988) for temperature and a classical single layer tank scheme (Hagemann and Stacke, 2015) for the water content in the root zone. Continuum runs operationally over the Italian territory as part of the monitoring and forecasting activities in support of the Italian Civil Protection. The model produces soil moisture maps at 500-m spatial resolution over the entire Italian territory and at a temporal resolution of 1 h. The outputs of this operational chain have been generated since 2008, and they were temporally aggregated at monthly scale as a simple average.

In order to compute the combined index, data from both SPEI-3 and SMA are aggregated over the municipalities, by averaging all the grid cells within a municipality that are classified as arable land according to the Corine land cover map, as presented in Fig. 1 (CLC2018, https://land.copernicus.eu/pan-european/corine-land-cover/clc2018).

2.3. Combining strategy

The proposed approach is based on the implementation of a double-entry matrix, where SPEI-3 and SMA data are the inputs, and a semi-quantitative classification of the drought severity is the output. As a basic principle, since both indices are standardized quantities aiming at capturing agricultural drought conditions, a symmetric matrix is considered both in terms of number of steps and threshold values. Specifically, a 5×5 matrix is here proposed, which requires the definition of four threshold values for each input index, and that allows to identify 25 double-entry combinations. In analogy to common classifications of drought severity (e.g., https://droughtmonitor.unl.edu/About/AbouttheData/DroughtClassification.aspx, last access 28/3/2023), five classes are considered for the combined indicator: D0) non-drought/wet conditions, D1) abnormally dry conditions, D2) moderate drought, D3) severe drought, D4)

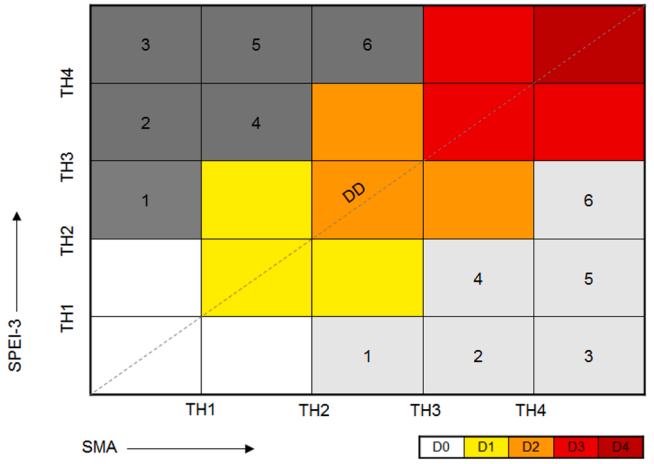

Fig. 2. Schematic representation of the double-entry matrix in relationship to SMA (x-axis) and SPEI-3 (y-axis) values. Cells along the diagonal (DD) represent agreement in drought class, whereas cells in the upper-left (UL, dark grey) and lower-right (LR, light grey) corners represent more extreme conditions reported by SPEI-3 and SMA, respectively. The number within each box highlights the mirrored combinations.

extreme drought. As for the thresholds, the values corresponding to the categories proposed by Agnew (2000) – TH = 0, − 0.84, − 1.28, − 1.65 – are investigated for both indices, which are based on common probability of occurrence values of standardized anomalies (probability of 0.5, 0.2, 0.1 and 0.05). Following the principle of the convergence of evidence (Leeper et al., 2022), and accounting for the similarities in both the physical meaning and the standardization procedure adopted for SPEI-3 and SMA, data from the two indices should ideally align along the diagonal of the matrix (DD, see Fig. 2), representing the conditions where the two indices converge in their assessment. Data in the upper-left corner (UL, dark grey in Fig. 2) represents all the conditions when SPEI-3 reports drier conditions than SMA, whereas the opposite occurs for the data in the lower-right corner (LR, light grey in Fig. 2).

The classification of drought for the combination along-diagonal (DD) is straightforward, since the two indices increase the drought severity proportionally, following the five classes previously defined (see color codes in Fig. 2), whereas the off-diagonal conditions need to be more carefully evaluated. To this end, we proposed an objective tuning strategy based on a two-phase method. First, the occurrence of such off-diagonal conditions is identified, and the periods, in which most of the discrepancies are concentrated, are isolated (i.e., high frequency of "outliers"). We used a minimum frequency of 15% to select the months when the 6 off-diagonal combinations are more frequent. Second, the most common along-diagonal classes under conditions similar to the "outliers" (in the surrounding municipalities) are used to assign the most-likely class in the corresponding off-diagonal combination. In this procedure, only the classes D1, D2, D3 along the diagonal (see Fig. 2) are considered, since the two most extreme classes, D0 and D4, can only be assigned when there is a strong convergence of the indices (less uncertainty) not possible in the off-diagonal cases.

In addition, since the drought classes have a decreasing frequency of occurrence due to their intrinsic probability definition (D1 is more frequent than D2, than D3), we used normalized frequencies rather than the absolute values to make the values comparable. Normalized frequencies were computed by diving the observed frequency in the subsets by the corresponding frequency values retrieved on the full dataset. According to this, drought classes are assigned to the 6 off-diagonal combinations (for both LR and UL classes).

This approach aims at maximizing the spatio-temporal consistency of the resulting classification, following the well-known smooth spatio-temporal dynamics of drought events (Hollins and Dodson, 2013), as well as to introduce a strategy that removes the arbitrariness in the matrix definition.

2.4. Reference impact records and evaluation metrics

Drought impact records from the updated version of the European drought impact report inventory (EDII, Blauhut et al., 2022; Stahl et al., 2016) are used to identify the major agricultural drought events in the two provinces over the period 2008–2019. The EDII is one of the most comprehensive archives of negative drought impacts as text-reports across Europe (Stahl et al., 2016). The data in Table 1 report the number of entries in the EDII for the entire Italian territory, as well as those specifically reporting Veneto/Verona or Apulia/Foggia.

These data clearly highlight the high number of entries for the years 2012, 2015 and 2017 (threefold or more than the other years), representing the years with the most spreading drought events. Despite their geographic separation, both provinces were affected by these three events, which indeed interested most of the Italian territory. Further evidence of the relevancy of the 2012 and 2017 droughts for the agriculture sector can be found in the declaration of natural calamity released by the Italian government (and specifically by the *Ministero delle Politiche Agricole, Alimentari e Forestali*, MIPAAF, https://www.politicheagricole.it), which allows for an economic compensation due to verified losses that exceed 30% of the production in those municipalities affected by droughts (Ministerial Decree April 18, 2008).

Table 1
Summary of the entries in the EDII database related to droughts in Italy in the period 2008–2009. In bold the years defined as "drought".

Year	Number of entries	Veneto/Verona	Apulia/Foggia
2008	4	no	yes
2011	7	no	no
2012	**61**	**yes**	**yes**
2013	16	no	no
2014	14	no	no
2015	**45**	**yes**	**yes**
2017	**87**	**yes**	**yes**
2019	10	no	no

We used this information as a reference to assess the performance of the combined index, by classifying each municipality into a binary system: "drought" or "non-drought" depending on the impact conditions reported in Table 1. The performance of the combined index is evaluated against this reference dataset by means of a confusion matrix, from which the four quantities true positive (TP), true negative (TN), false positive (FP) and false negative (FN) can be derived. The overall behaviour of the combined index can be synthetically described by few statistical metrics:

$$FAR = \frac{FP}{TP + FP} \tag{1}$$

the false alarm ratio (FAR), namely the fraction of the modelled events that are false alarms. This metric ranges from 0 to 1, with 0 being the best score.

$$POD = \frac{TP}{TP + FN} \tag{2}$$

the probability of detection (POD), which represents the fraction of the observed events that are correctly modelled. It ranges from 0 to 1, with 1 representing the best score.

$$ACC = \frac{TP + TN}{TP + TN + FP + FN} \tag{3}$$

The accuracy (ACC), which is the fraction of the total events correctly modelled. This metric has also a best score at 1.

$$HSS = \frac{2(TP \cdot TN - FP \cdot \mathrm{FN})}{[(\mathrm{TP} + \mathrm{FN})(\mathrm{FN} + \mathrm{TN}) + (\mathrm{TP} + \mathrm{FP})(\mathrm{FP} + \mathrm{TN})]} \tag{4}$$

the Heidke skill score (HSS), summarising the overall modelling skill of the index. This metric is lower than 0 when the model has no skill, and equal to 1 for the perfect model.

The first two metrics, FAR and POD, highlight the capability of the index to both minimise false alarms while simultaneously detecting the reference events, whereas the ACC and HSS metrics focus on the overall capability of the index to capture the recorded drought events.

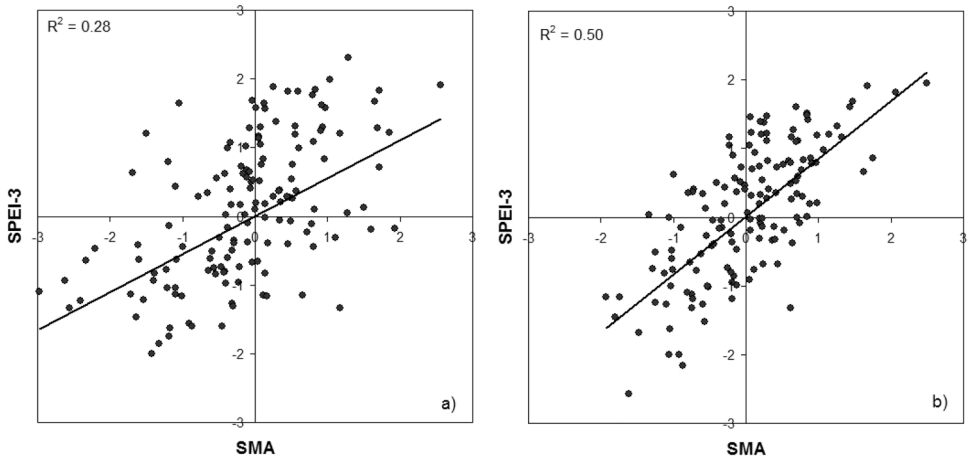

Fig. 3. Scatterplot between province-average SMA and SPEI-3 data for: a) Verona, and b) Foggia provinces during the period 2008–2019.

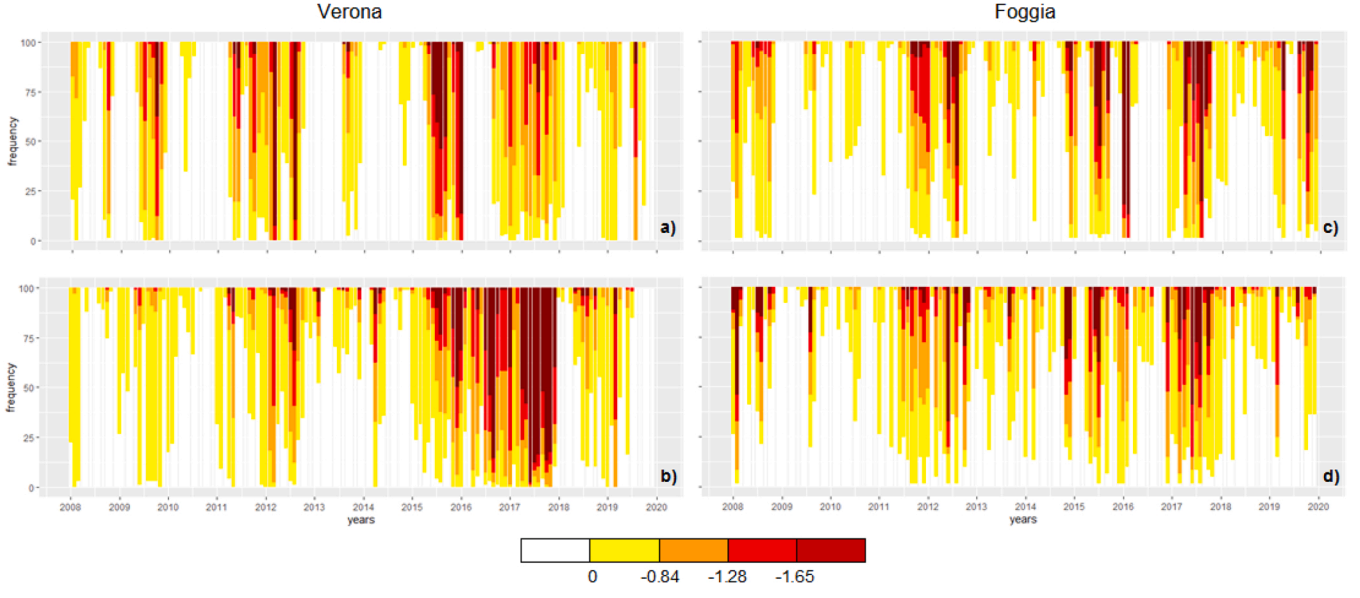

Fig. 4. Fraction of municipalities (frequency, %) in the provinces of Verona (left column panels) and Foggia (right column panels) with SPEI-3 (a,c) or SMA (b,d) values within the five drought classes.

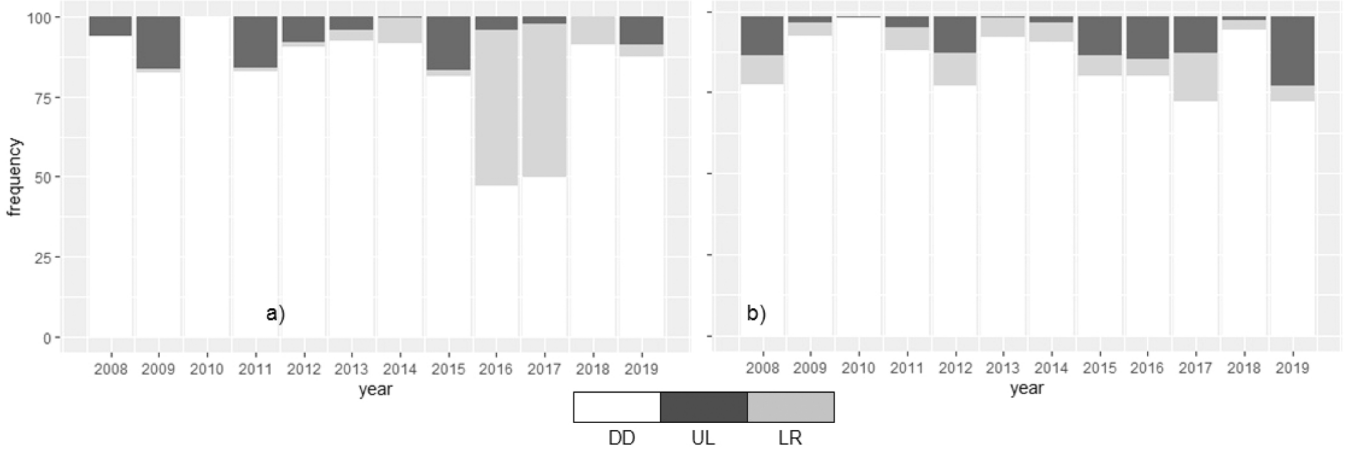

Fig. 5. Data frequency on the three categories in the double-entry matrix (see Fig. 2): DD, along the diagonal, UL, upper-left corner, and LR, lower-right corner, for the provinces of Verona (panel a) and Foggia (panel b).

class	avg	1	2	3	4	5	6
D0	59.4	0.51	0.28	0.16	0.06	0.04	0.00
D1	16.5	**0.87**	**0.20**	**0.19**	1.68	0.66	0.28
D2	4.2	0.44	0.11	0.12	**3.89**	**2.30**	2.26
D3	3.0	0.13	0.00	0.00	1.26	2.20	**7.47**
D4	1.1	0.12	0.00	0.00	1.53	4.66	7.34

Fig. 6. Summary of the normalized frequency for the classes D0-D4 computed on the subset of months with a high frequency (> 15%) of each of the 6 off-diagonal combinations (see the codes reported in Fig. 2). The normalization is performed with the corresponding average frequency (avg) computed on the entire dataset (pooling together data from the two provinces). The higher value for D1-D3 in each of the 6 combinations is highlighted in bold and colored with the corresponding drought class.

3. Results

3.1. Setting up of the double-entry matrix

The agreement between the two selected drought indices, as a basic assumption of the convergence of evidence principle, is first tested on the spatially averaged values of the two provinces separately (Fig. 3). Data between 2008 and 2019 are used, for a total of 144 monthly values for each province. The scatterplots between SPEI-3 and SMA show statistically significant values of the coefficient of determination (R^2, significant at $p < 0.01$) for both provinces, confirming the overall coherence of the two indices. A residual unexplained variance is still clearly visible in both scatterplots (i.e., dispersion around the regression line), suggesting the potential added value of the combined index, since these are the conditions where the two indices somehow disagree on their individual values (see scheme in Fig. 2).

Next, the temporal coherence of the drought assessments by the two indices is tested by computing the time series of the fraction of municipalities within five drought classes: (> 0, < 0, < -0.84, < -1.28, < -1.65), as reported in Fig. 4 for the two provinces (Fig. 4a,c for SPEI-3; b,c for SMA). Since all the municipalities are assigned to one of the five classes, all the frequencies sum up to 100% of the territory for each time period.

An overall coherence between the time series of the two indices can be observed for both provinces, with a higher density of dark shades (i.e., moderate to extreme drought conditions) in correspondence of the documented droughts of 2012, 2015 and 2017. With dry conditions for the event in 2012 starting as early as the end of 2011, whereas the 2015 event occurred mostly during summer months. The event of 2017 is confirmed to be the most severe of the study period, with an intense summer drought preceded by a dry winter and a similarly dry late 2016.

Besides the overall similarities between the plots for the two indices, some discrepancies can also be observed, such as, for instance, the SMA dry anomalies observed in 2014 for Verona (Fig. 4b). These instances of disagreement are the focus of the successive analysis, where the frequency of the inconsistencies between the two indices is quantified by discriminating for each year the combinations that

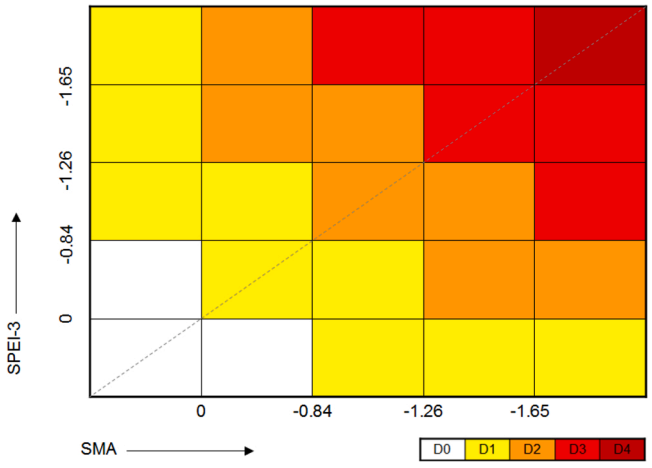

Fig. 7. Proposed double-entry matrix for the combination of the combined index, tuned on the data obtained for the two study cases.

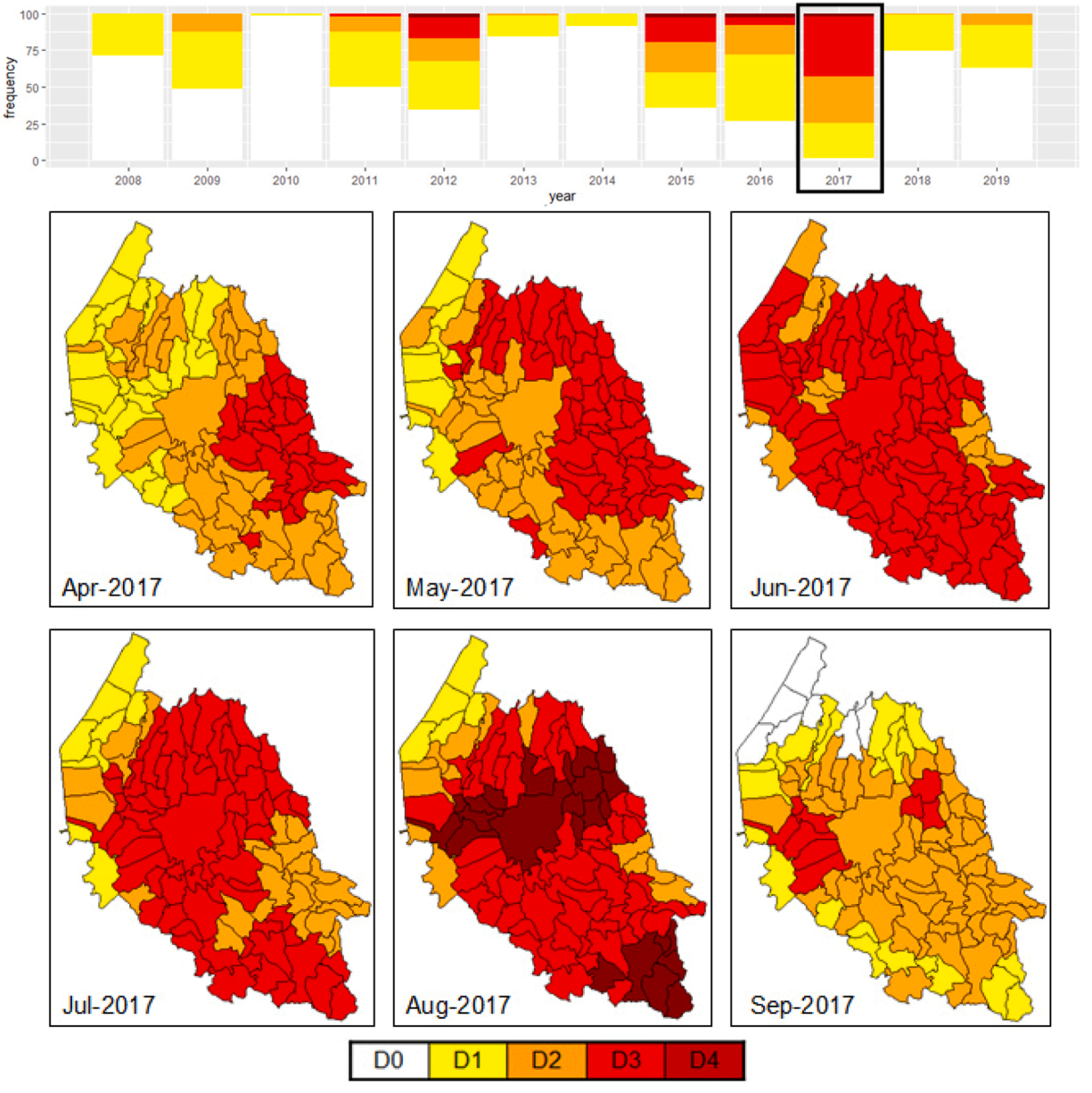

Fig. 8. Time series of the annually-aggregated drought classes for the province of Verona (top panel), and drought severity maps based on the proposed combined index for the drought event in Verona province April-September 2017.

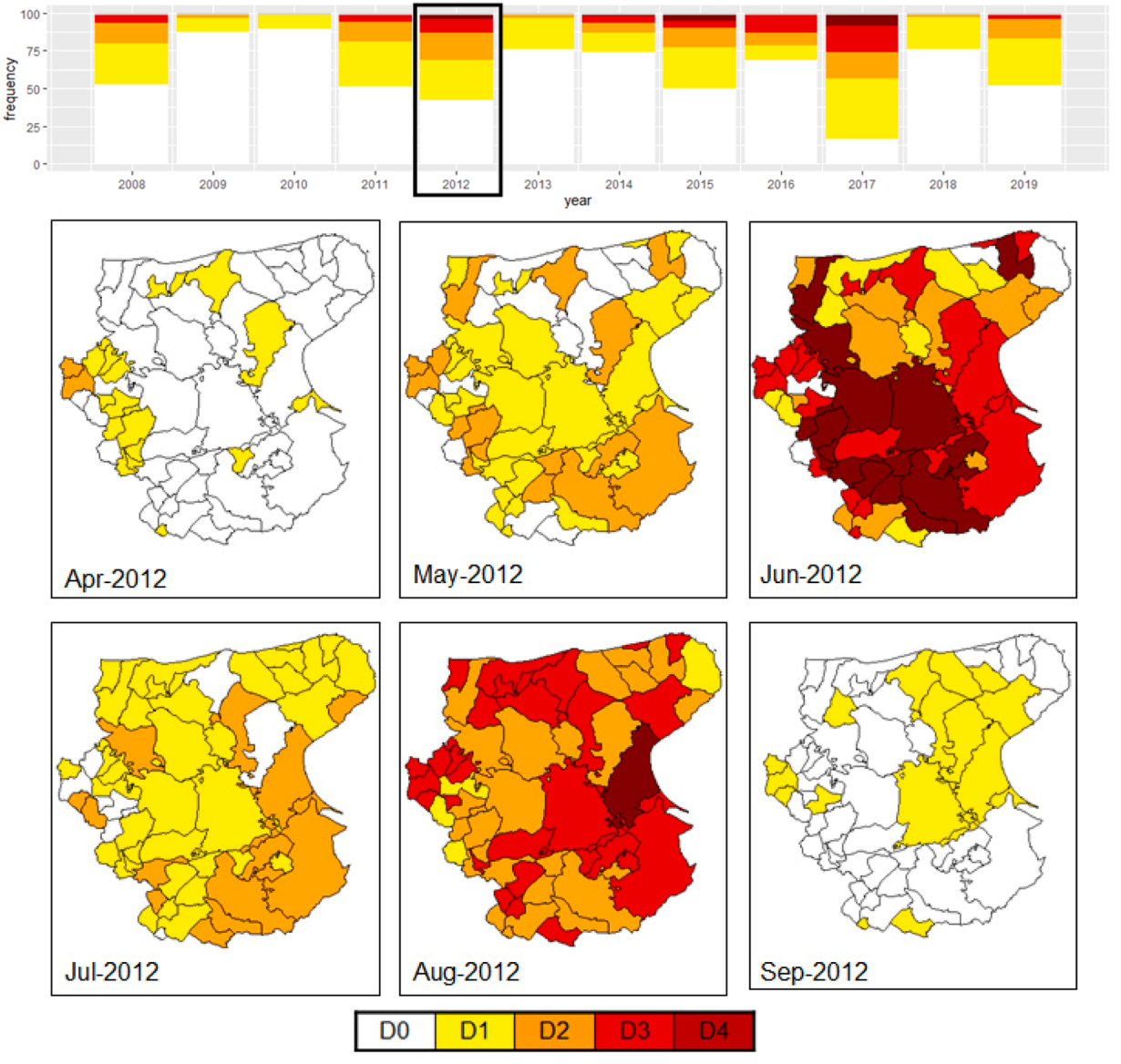

Fig. 9. Time series of the annually-aggregated drought classes for the province of Foggia (top panel), and drought severity maps based on the proposed combined index for the drought event in Foggia province April-September 2012.

fall into the three categories DD (pooled together in a single category), UL and LR in the double-entry matrix (see Fig. 2 for details).

The plots in Fig. 5 reports the results for Verona (panel a) and Foggia (panel b), highlighting the years where most of the discrepancies are located. A general outcome of this analysis is a slight tendency to observe larger frequencies in the LR classes compared to the UL ones. The average frequency in the UL class is 7.2%, whereas the frequency in the LR class is 8.5%. These results further underline the tendency of SMA to return more severe values already observed in Fig. 4.

Larger discrepancies are observed for the Verona province (Fig. 5a) compared to Foggia, a result mainly driven by the high frequency of LR cases observed in the drought years 2016 and 2017. This result is in line with the lower R^2 value observed for the province of Verona compared to Foggia, which corresponds to a higher disagreement between the two indices. The discrepancies are more evenly distributed among the different years for the Foggia province, although also in this case it is possible to notice a higher frequency during 2016 and 2017, but with a more uniform distribution between UL and LR cases in 2017.

The results reported in Fig. 5 allow us to focus on specific periods where most of the discrepancies are concentrated, and to separate the municipalities with divergent results from the ones where the two indices agree. For this analysis, we selected the years with the highest frequency of cases in LR or UL classes, such as: 2009, 2015 (high frequency of UL), 2016 and 2017 (high frequency of LR) for Verona, and 2008 (high frequency of LR), 2016 (high frequency of UL), 2012, and 2017 (high frequency of both UL and LR) for Foggia.

In order to assign a drought class to the 6 off-diagonal combinations represented in Fig. 2 (for both LR and UL classes), we firstly identified the months when those conditions are more frequent during the selected years using the minimum frequency of 15%. Subsequently, only for this selected subset, we extracted the municipalities with values in the D1, D2, D3 classes along the diagonal (see Fig. 2) and we computed their normalized frequency values.

The data in Fig. 6 summarize the values obtained for these normalized frequencies by pooling together the two provinces, since a single parameterization of the double-entry matrix is searched. For each of the 6 off-diagonal combinations the highest normalized frequency value is highlighted in bold, and the corresponding color-coded drought class is reported.

These results show a smooth transition from the D1 class selected for the combinations 1–3, corresponding to the cases were one the two base indices have positive values, to the class D2 for the combinations 4 and 5, up to the class D3 for the combination 6 (corresponding to the cases where one of the two base indices has a value lower than the maximum threshold −1.65). By adding these results to the preliminary matrix introduced in Fig. 2, we obtained the final double-entry matrix to be used for the computation of the combined index, which is reported in Fig. 7.

3.2. *Performance during agricultural drought events*

The proposed double-entry matrix is applied to the full time series of data available for the two provinces in order to evaluate the temporal evolution of the frequency of the five drought classes during the entire study period. The plots on top of Figs. 8 and 9 clearly show 2017 as the year with the highest frequency of combined D2-D4 classes for both provinces. This result was expected from the impacts recorded for that year in the agriculture sector, followed by 2012 for the Foggia province and by 2015 and 2012 for the Verona province.

A qualitative analysis of the temporal evolution of the combined index for the two drought years 2012 and 2017 can be performed on the maps depicting the index over each municipality for the main growing season (April to September) for the Verona province in 2017 (Fig. 8), and for the Foggia province in 2012 (Fig. 9). These two years are selected as those in which the MIPAAF reported the major impacts for the agricultural sector in the most recent years.

The relevancy of the drought conditions for these two growing seasons is well captured by the combined index in both case studies, with maps that display the maximum severity class (D4: extreme drought) over some municipalities in August 2017, June 2012, and August 2012. Overall, the index is able to identify the drought of 2017 as the more persistent of the two, with a smooth transition between different classes, starting with a predominance of municipalities in D2 in April 2017 and reaching its peak between June and August, when most of the municipalities experienced D3 or D4 drought conditions. Finally, a statistical analysis of the combined index is performed by converting the modelled data in a set of binary “drought” and “non-drought” values, in analogy to the reference dataset (see Section 2.4). For each municipality, we considered a “drought” year when the combined index was classified as D3 or D4 in at least one month of the period April-September (average growing season of the two regions), or as “non-drought” year otherwise. Then, a set of statistical metrics are computed by comparing the reference and the modelled values though a confusion matrix (see Section 2.4). The values obtained for the statistical metrics are summarized in Table 2.

Overall, the proposed method is proven to be skillful in detecting the occurrence of drought (Heidke Skill Score, HSS = 0.75), with high values of both Probability of Detection (POD = 0.80) and Accuracy (ACC = 0.90), as well as a relatively low value of the False Alarm Ratio (FAR = 0.18). The data in Table 2 show also the improvement obtained over the use of the two single indices separately, which is mostly visible in HSS, due to the reduction in false alarms thanks to the converge of evidence.

4. Discussion

Preliminary analyses on the spatio-temporal behavior of SPEI-3 and SMA, separately, show the expected overall consistency. This result supports the use of the two indices as input for the double-entry matrix, since the evidence of extreme conditions seems to converge. Overall, the correlation between SPEI-3 and SMA is higher for Foggia, which can be explained by the more straightforward connection between precipitation-evapotranspiration and soil moisture in a water-controlled environment such as the ones in Mediterranean climate compared to the more water-rich conditions of north-eastern Italy.

The overall good consistency observed in the correlation is also valid for the detection of drought events by the two indices. As few

Table 2
Summary of the statistical metrics derived by comparing the reference drought years against the modelled values.

Metric	Verona			Foggia			Verona + Foggia		
	SPEI-3	SMA	combined	SPEI-3	SMA	combined	SPEI-3	SMA	combined
POD	0.91	0.68	0.80	0.91	0.84	0.81	0.91	0.74	0.80
FAR	0.42	0.48	0.19	0.30	0.42	0.17	0.37	0.46	0.18
ACC	0.81	0.76	0.90	0.88	0.81	0.91	0.84	0.78	0.90
HSS	0.56	0.43	0.74	0.71	0.56	0.76	0.62	0.48	0.75

POD: Probability of Detection (1 is best); FAR: False Alarm Ratio (0 is best); ACC: Accuracy (1 is best); HSS: Heidke Skill Score (> 0 is skillful).

examples, for the event of 2012, dry conditions started as early as the end of 2011 for both SPEI-3 and SMA, before reaching a peak during summer 2012. In 2015, the severity of the drought seems less marked than in the other two drought years, and mostly characterized by a short and intense peak around summer of that year, whereas for the event of 2017, summer drought conditions followed a dry winter and a similarly dry 2016.

The analysis of the temporal dynamics of the area under drought shows a tendency of SMA to report more extreme anomalies compared to SPEI-3, especially for the Verona province (Fig. 4). This behavior can be explained by the longer memory of soil moisture compared to precipitation, as two consecutive dry winters (2016 and 2017) seem to have caused soil moisture dryness already in early 2017. Another possible explanation of the more extreme values observed in SMA can be the aggregation of SPEI over a 3-month period, which tends to smooth isolated extreme conditions.

While the discrepancies between the two indices are rather limited (in the order of 15% of all the cases), they can reach up to 50% in some extreme cases (e.g., Verona in 2016 and 2017). The arbitrariness in defining a severity class corresponding to these off-diagonal combinations (in case of indices with comparable range of variability and analogous physical meaning) is limited by the introduction of objective optimization approaches, overcoming the limitations of arbitrarily defined weighting factors as in Balint et al. (2013), or the use of factors based on expert responses' (Bravo et al., 2021).

The resulting double-entry matrix suggests a smooth transition between the different severity classes, similarly to many standard risk matrices used in a variety of fields, such as the one used by NASA in the risk management process in a project lifecycle (Seasly, 2018), or by the Department of Defense (DoD, 2017). However, in this case the intrinsic subjectivity in defining the classes (Redmill, 2002) is circumvented using a reproducible methodology based on the data collected in the test cases. By using the same classes for the combinations corresponding to the mirrored conditions in the UL and LR corners of the matrix (e.g., the two combinations 6 in Fig. 2), the proposed solution maintains the symmetric feature required by the physical definition of the two base indicators even without any a-priori constrain imposed in this regard.

The application of this methodology to the two study areas not only leads to good performance in terms of skill of the assessment, but also a characterization of spatio-temporal evolution of two well-documented past droughts. This is in line with the characterization of drought based on the scientific literature and impact records. As an example, the presence of large areas with D2 (or higher) already in April for the event of 2017 over Verona is well supported by a prolonged lack of rain that started as early as during autumn 2016, and propagated throughout 2017. In the case of the 2012 drought over the Foggia province, the drought was mainly triggered by a sequence of heat-waves of various intensity that invested southern Europe between May and September, with the only two months with severe rainfall deficits being June and August. This is well reflected in the dynamic of the combined indicator for the Foggia province, which shows two pronounced peaks in the drought severity in June and August, but also an overall shorter duration of the drought compared to the one in 2017 over the Verona province.

The improved skill of the combined index compared to the base inputs has been observed also by Kavianpour et al. (2018) in analyzing the performance of a copula-based index over Iran. Faiz et al. (2022) highlighted similar improvements in the performance of a combined precipitation, soil moisture and evapotranspiration index due to the reduction of false alarm ratio, a result that is also supported by the present outcomes. A better capability of a combined index to capture drought effects on foodgrain production compared to base indices based on precipitation, streamflow or vegetation health was observed over India by Prajapati et al. (2022). Even if no direct comparison with yield or production data was possible in this experiment, the good agreement with the qualitative information on impacts derived from both drought impact records and the declaration of natural calamity for the Italian government seems to support a similar outcome for the proposed index.

In addition to the good performances over the two case studies, the proposed methodology has the advantage of being based on a simple approach, which is not computationally expensive and that can be then easily implemented operationally in a near-real time monitoring system. The structure of the double-entry matrix facilitates the backtracking of the conditions that produced a specific class, which can be exploited by expert user to further understand the development of specific droughts and the causes that generated such conditions.

5. Conclusions

The assessment of drought conditions at national- and sub-national spatial scales is of vital importance not only for the estimation of damage compensation, but also to enhance the preparedness of a territory in case of upcoming natural disasters.

The use of combined indices represents an invaluable resource to overcome the limitations of simple drought indices, and, in particular, the double-entry matrices constitute a flexible tool suitable for operational applications. The procedure proposed in this

study to set-up the double-entry matrix introduces an objective and replicable approach that bases the classification of the combination under disagreement using the contemporary conditions observed in the cases with agreement.

The reliability of this procedure is supported by the results obtained for the two study cases of Verona and Foggia provinces, where a realistic representation of the major agricultural droughts events of 2012, 2015 and 2017 was obtained, with a high skill compared to the narrative reported by past impact records. The simplicity and skillfulness of the methodology showed great potential for upscaling at national level in an operational monitoring context, and the outcomes of this study support the development of a monitor system for agricultural drought to trigger drought management actions during the growing season, as well as to identify municipalities affected by drought to activate possible damage compensation actions.

CRediT authorship contribution statement

Lauro Rossi: Conceptualization, Data curation, Formal analysis, Methodology, Investigation, Writing – original draft, Writing – review & editing. **Gustavo Naumann:** Conceptualization, Data curation, Formal analysis, Methodology, Investigation, Writing – original draft, Writing – review & editing. **Simone Gabellani:** Conceptualization, Data curation, Formal analysis, Methodology, Investigation, Writing – original draft, Writing – review & editing. **Carmelo Cammalleri:** Conceptualization, Data curation, Formal analysis, Methodology, Investigation, Writing – original draft, Writing – review & editing.

Declaration of Competing Interest

The authors declare that they have no known competing financial interests or personal relationships that could have appeared to influence the work reported in this paper.

Data Availability

Data will be made available on request.

Appendix A. Supporting information

Supplementary data associated with this article can be found in the online version at doi:10.1016/j.ejrh.2023.101404.

References

Agnew, C.T., 2000. Using the SPI to identify drought. Drought Network News (1994–2001) 12(1): 1–12, ⟨http://digitalcommons.unl.edu/droughtnetnews/1⟩. [last access: November 2022].

Alley, W.M., 1984. The Palmer Drought Severity Index: limitations and assumptions. J. Appl. Meteor. 23, 1100–1109. https://doi.org/10.1175/1520-0450(1984)023<1100:TPDSIL>2.0.CO;2.

Anderson, M.C., Hain, C.R., Wardlow, B., Mecikalski, J.R., Kustas, W.P., 2011. Evaluation of a drought index based on thermal remote sensing of evapotranspiration over the continental U.S. J. Clim. 24, 2025–2044. https://doi.org/10.1175/2010JCLI3812.1.

Balint, Z., Mutua, F., Muchiri, P., Omuto, C.T., 2013. Monitoring drought with the combined drought index in Kenya. Dev. Earth Surf. Process 16, 341–356. https://doi.org/10.1016/B978-0-444-59559-1.00023-2.

Blauhut, V., Stephan, R., Stahl, K., 2022. The European Drought Impact Report Inventory (EDII V2.0). Version 2.0. ⟨https://doi.org/10.6094/UNIFR/230922⟩.

Braca, G., Bussettini, M., Lastoria, B., Mariani, S., Piva, F., 2021. Elaborazioni modello BIGBANG versione 4.0. Istituto Superiore per la Protezione e la Ricerca Ambientale – ISPRA, ⟨http://groupware.sinanet.isprambiente.it/bigbang-data/library/bigbang40⟩.

Bravo, R.Z.B., Cunha, A.P.Md, Leiras, A., Cyrino Oliveira, F.L., 2021. A new approach for a drought composite index. Nat. Hazards 108, 755–773. https://doi.org/10.1007/s11069-021-04704-x.

Cammalleri, C., Micale, F., Vogt, J., 2016. A novel soil moisture-based drought severity index (DSI) combining water deficit magnitude and frequency. Hydrol. Process. 30, 289–301. https://doi.org/10.1002/hyp.10578.

Cenci, L., Laiolo, P., Gabellani, S., Campo, L., Silvestro, F., Delogu, F., Boni, G., Rudari, R., 2016. Assimilation of H-SAF soil moisture products for flash flood early warning systems. case study: Mediterranean catchments. IEEE J. Sel. Top. Appl. Earth Obs. Remote Sens. 9 (12), 5634–5646. https://doi.org/10.1109/JSTARS.2016.2598475.

Corral, C., Berenguer, M., Sempere-Torres, D., Poletti, L., Silvestro, F., Rebora, N., 2019. Comparison of two early warning systems for regional flash flood hazard forecasting. J. Hydrol. 572, 603–619. https://doi.org/10.1016/j.jhydrol.2019.03.026.

Crow, W.T., Kumar, S.V., Bolten, J.D., 2012. On the utility of land surface models for agricultural drought monitoring. Hydrol. Earth Syst. Sci. 16, 3451–3460. https://doi.org/10.5194/hess-16-3451-2012.

De Stefano, L., Fornés, J.M., López-Geta, J.A., Villarroya, F., 2015. Groundwater use in Spain: an overview in light of the EU water framework directive. Int. J. Water Resour. Dev. 31 (4), 640–656. https://doi.org/10.1080/07900627.2014.938260.

Department of Defense, 2017. Risk, Issue, and Opportunity Management Guide for Defense Acquisition Programs, Washington DC, 96 pp. Available at: ⟨https://acqnotes.com/wp-content/uploads/2017/07/DoD-Risk-Issue-and-Opportunity-Management-Guide-Jan-2017.pdf⟩ [last access: November 2022].

Dickinson, R.E., 1988. The force-restore model for surface temperatures and its generalizations. J. Clim. 1 (11), 1086–1097. ⟨https://www.jstor.org/stable/44363960⟩.

Faiz, M.A., Zhang, Y., Zhang, X., Ma, N., Aryal, S.K., Ha, T.T.V., Baig, F., Naz, F., 2022. A composite drought index developed for detecting large-scale drought characteristics. J. Hydrol. 605, 127308 https://doi.org/10.1016/j.hydrol.2021.127308.

Food and Agriculture Organization of the United Nations (FAO), 2021. The impact of disasters and crises on agriculture and food security: 2021, Rome, Italy, 245 pp. Available at: ⟨https://doi.org/10.4060/cb3673en⟩ [last access: November 2022].

García-León, D., Standardi, G., Staccione, A., 2021. An integrated approach for the estimation of agricultural drought costs. Land Use Policy 100, 104923. https://doi.org/10.1016/j.landusepol.2020.104923.

Hagemann, S., Stacke, T., 2015. Impact of the soil hydrology scheme on simulated soil misture memory. Clim. Dyn. 44, 1731–1750. https://doi.org/10.1007/s00382-014-2221-6.
Hao, Z., AghaKouchak, A., 2013. Multivariate Standardized Drought Index: a parametric multi-index model. Adv. Water Resour. 57, 12–18. https://doi.org/10.1016/j.advwatres.2013.03.009.
Hoffmann, D., Gallant, A.J.E., Arblaster, J.M., 2020. Uncertainties in drought from index and data selection. JGR Atmos. 125 (18), e2019JD031946 https://doi.org/10.1029/2019JD031946.
Hollins, S., Dodson, J., 2013. Drought. In: Bobrowsky, P.T. (Ed.), Encyclopedia of Natural Hazards. Encyclopedia of Earth Sciences Series. Springer, Dordrecht, pp. 189–197. https://doi.org/10.1007/978-1-4020-4399-4_98.
Jordan, S., Mitterhofer, H., Jørgensen, L., 2018. The interdiscursive appeal of risk matrices: Collective symbols, flexibility normalism and the interplay of 'risk' and 'uncertainty'. Account. Organ. Soc. 67, 34–55. https://doi.org/10.1016/j.aos.2016.04.003.
Kavianpour, M., Seyedabadi, M., Moazami, S., 2018. Spatial and temporal analysis of drought based on a combined index using copula. Environ. Earth Sci. 77, 769. https://doi.org/10.1007/s12665-018-7942-0.
Kogan, F.N., 1995. Application of vegetation index and brightness temperature for drought detection. Adv. Space Res. 15 (11), 91–100.
Laiolo, P., Gabellani, S., Campo, L., Silvestro, F., Delogu, F., Rudari, R., Pulvirenti, L., Boni, G., Fascetti, F., Pierdicca, N., Crapolicchio, R., Hasenauer, S., Puca, S., 2016. Impact of different satellite soil moisture products on the predictions of a continuous distributed hydrological model. International Journal of Applied Earth Observation and Geoinformation 48, 131–145. https://doi.org/10.1016/j.jag.2015.06.002. ISSN 1569-8432.
Leeper, R.D., Bilotta, R., Petersen, B., Stiles, C.J., Heim, H., Fuchs, B., Prat, O.P., Palecki, M., Ansari, S., 2022. Characterizing U.S. drought over the past 20 years using the U.S. drought monitor. Int. J. Climatol. 42 (12), 6616–6630. https://doi.org/10.1002/joc.7653.
McKee, T.B., N.J. Doesken and J. Kleist, 1993. The Relationship of Drought Frequency and Duration to Time Scales. Proceedings of the 8th Conference on Applied Climatology, 17–22 January 1993, Anaheim, CA. Boston, MA, American Meteorological Society.
Meza, I., Siebert, S., Döll, P., Kusche, J., Herbert, C., Rezaei, E.E., Nouri, H., Gerdener, H., Popat, E., Frischen, J., Naumann, G., Vogt, J.V., Walz, Y., Sebesvari, Z., Hagenlocher, M., 2020. Global-scale drought risk assessment for agricultural systems. Nat. Hazards Earth Syst. Sci. 20, 695–712. https://doi.org/10.5194/nhess-20-695-2020.
Naumann, G., Spinoni, J., Vogt, J.V., Barbosa, P., 2015. Assessment of drought damages and their uncertainties in Europe. Environ. Res. Lett. 10, 124013 https://doi.org/10.1088/1748-9326/10/12/124013.
Peng, J., Muller, J.-P., Blessing, S., Giering, R., Danne, O., Gobron, N., Kharbouche, S., Ludwig, R., Müller, B., Leng, G., You, Q., Duan, Z., Dadson, S., 2019. Can we use satellite-based FAPAR to detect drought? Sensors 19, 3663. https://doi.org/10.3390/s19173662.
Poletti, M.L., Silvestro, F., Davolio, S., Pignone, F., Rebora, N., 2019. Using nowcasting technique and data assimilation in a meteorological model to improve very short range hydrological forecasts. Hydrol. Earth Syst. Sci. 23, 3823–3841. https://doi.org/10.5194/hess-23-3823-2019.
Prajapati, V.K., Khanna, M., Singh, M., Kaur, R., Sahoo, R.N., Singh, D.K., 2022. PCA-based composite drought index for drought assessment in Marathwada region of Maharashtra state, India. Theor. Appl. Climatol. 149, 207–220. https://doi.org/10.1007/s00704-022-04044-1.
Redmill, F., 2002. Risk analysis - A subjective process. Eng. Manag. 12 (2), 91–96. https://doi.org/10.1049/em:20020206.
Riha, S.J., Wilks, D.S., Simoens, P., 1996. Impact of temperature and precipitation variability on crop model predictions. Clim. Change 32, 293–311. https://doi.org/10.1007/BF00142466.
Seasly, E.E., 2018. Methodology to Evaluate Proposed Leading Indicators of Space System Performance Degradation Due to Contamination. PhD dissertation, George Washington University, 123 pp. Available at: ⟨https://www.researchgate.net/publication/324896786_Methodology_to_Evaluate_Proposed_Leading_Indicators_of_Space_System_Performance_Degradation_Due_to_Contamination⟩. [last access: November 2022].
Sheffield, J., Wood, E.F., 2007. Characteristics of global and regional drought, 1950–2000: analysis of soil moisture data from off-line simulation of the terrestrial hydrologic cycle. J. Geophys. Res. Atmos. 112 (D17) https://doi.org/10.1029/2006JD008288.
Silvestro, F., Gabellani, S., Delogu, F., Rudari, R., Boni, G., 2013. Exploiting remote sensing land surface temperature in distributed hydrological modelling: the example of the Continuum model. Hydrol. Earth Syst. Sci. 17, 39–62. https://doi.org/10.5194/hess-17-39-2013.
Silvestro, F., Gabellani, S., Delogu, F., Rudari, R., Laiolo, P., Boni, G., 2015. Uncertainty reduction and parameter estimation of a distributed hydrological model with ground and remote-sensing data. Hydrol. Earth Syst. Sci. 19, 1727–1751. https://doi.org/10.5194/hess-19-1727-2015.
Silvestro, F., Rebora, N., Rossi, L., Dolia, D., Gabellani, S., Pignone, F., Trasforini, E., Rudari, R., De Angeli, S., Masciulli, C., 2016. What if the 25 October 2011 event that struck Cinque Terre (Liguria) had happened in Genoa, Italy? flooding scenarios, hazard mapping and damage estimation. Nat. Hazards Earth Syst. Sci. 16, 1737–1753. https://doi.org/10.5194/nhess-16-1737-2016.
Silvestro, F., Rossi, L., Campo, L., Parodi, A., Fiori, E., Rudari, R., Ferraris, L., 2019. Impact-based flash-flood forecasting system: Sensitivity to high resolution numerical weather prediction systems and soil moisture. J. Hydrol. Volume 572, 388–402. https://doi.org/10.1016/j.jhydrol.2019.02.055.
Stahl, K., Kohn, I., Blauhut, V., Unquijo, J., De Stefano, L., Acácio, V., Dias, S., Stagge, J.H., Tallaksen, L.M., Kampragou, E., Van Loon, A.F., Barker, L.J., Melsen, L.A., Bifulco, C., Musolino, D., de Carli, A., Massarutto, A., Assimacopoulos, D., Van Lanen, H.A.J., 2016. Impacts of European drought events: insights from an international database of text-based reports. Nat. Hazards Earth Syst. Sci. 16, 801–819. https://doi.org/10.5194/nhess-16-801-2016.
Thornthwaite, C.W., 1948. An approach toward a rational classification of climate. Geogr. Rev. 38 (1), 55–94. https://doi.org/10.2307/210739.
UNDRR (United Nations Office for Disaster Risk Reduction), 2021. GAR Special Report on Drought 2021. Geneva, 210 pp.
Venezian Scarascia, M.E., Di Battista, F., Salvati, L., 2006. Water resources in Italy: availability and agricultural uses. Irrig. Drain. 55, 115–127. https://doi.org/10.1002/ird.222.
Vicente-Serrano, S.M., Santiago Beguería, J., López-Moreno, I., 2010. A Multi-scalar drought index sensitive to global warming: the Standardized Precipitation Evapotranspiration Index - SPEI. J. Clim. 23, 1696–1718. https://doi.org/10.1175/2009JCLI2909.1.
World Meteorological Organization, 2017. Guidelines on the Calculation of Climate Normals (WMO-No. 1203), Geneva.
World Meteorological Organization (WMO) and Global Water Partnership (GWP), 2014. National Drought Policy Guidelines: A Template for Action, D.A. Wilhite, ed. Integrated Drought Management Programme Tools and Guidelines Series 1. Geneva and Stockholm, 48 pp. Available at: ⟨https://www.droughtmanagement.info/literature/IDMP_NDMPG_en.pdf⟩ [last access: November 2022].
World Meteorological Organization (WMO) and Global Water Partnership (GWP), 2016. Handbook of Drought Indicators and Indices (M. Svoboda and B.A. Fuchs). Integrated Drought Management Programme (IDMP), Integrated Drought Management Tools and Guidelines Series 2. Geneva, 52 pp. Available at: ⟨https://www.droughtmanagement.info/literature/GWP_Handbook_of_Drought_Indicators_and_Indices_2016.pdf⟩ [last access: November 2022].